

## Experimental study at prototype scale of a self-priming free surface siphon

### *Etude expérimentale à l'échelle prototype d'un siphon auto-amorçant à surface libre*

Giovanni De Cesare<sup>1</sup>, Khalid Essyad<sup>2</sup>, Paloma Furlan<sup>3</sup>, Vu Nam Khuong<sup>4</sup>, Sean Mulligan<sup>5</sup>

<sup>1</sup>EPFL, LCH, Station 18, 1015 Lausanne, Switzerland  
giovanni.decesare@epfl.ch

<sup>2</sup>BG Ingénieurs Conseils, Eau & Environnement, Av. de Cour 61, CP 241, 1001 Lausanne, Switzerland, khalid.essyad@bg-21.com

<sup>3</sup>EPFL, LCH, Station 18, 1015 Lausanne, Switzerland  
paloma.furlan@epfl.ch

<sup>4</sup>BG Ingénieurs Conseils, Eau & Environnement, Av. de Cour 61, CP 241, 1001 Lausanne, Switzerland, vunam.khuong@bg-21.com

<sup>5</sup>National University of Ireland, Department of Civil Engineering, Gaillimh, Co. Galway, Ireland  
seanmulligan23@gmail.com

## KEY WORDS

Vortex, air entrainment, negative pressure, free surface, water transfer, groundwater

## ABSTRACT

*This study is within the frame of the construction of the rail link between Geneva Cornavin station, Eaux-Vives station and Annemasse (CEVA). The project area is located at a cut-and-cover tunnel built by slurry walls located in the alluvium of the Foron River. The installation of the covered trench cuts the groundwater flow, which causes a rise of the water table in spite of the partial evacuation by the Foron. It is therefore planned to add about thirty wells in order to transit the waters of the aquifer from one side of the tunnel to the other. A thorough reflection allowed to find an alternative solution to traditional pumping consisting of putting in place self-priming multiphase siphons which forms the basis of the following study. The operating principle of the system is based on the maintenance of a free-surface vortex in a vacuum in what will be called the sealed box which functions by keeping the siphon primed to allow water to be transferred from either side of the gallery. This study explores the performance of a physical model of the system with the following objectives: (1) To characterize the initiation and stability conditions of the system by maintaining the vacuum in the sealed box and (2) to characterize the limiting operating conditions of the system in relation to the ground water table levels which relates to insufficient air entrainment due to low outflow or submergence of the sealed box. The experimental installation is fabricated at a scale of 1:1 so as not to introduce scale effects by the presence of air, the water-air mixture and the free-surface vortex in a vacuum atmosphere.*

## 1. INTRODUCTION

CEVA (Cornavin–Eaux-Vives–Annemasse) is a 16 km long orbital city rail line which was designed to connect the Geneva main station Cornavin with the French Annemasse train station to the south via the Gare des Eaux-Vives. When completed, the link will allow through running between the main

---

<sup>1</sup> Corresponding author: giovanni.decesare@epfl.ch

Swiss rail network and the isolated line east of Annemasse in Haute-Savoie. CEVA will run inside double track line tunnels.

The last section between Gare des Eaux-Vives and the Swiss-French border encounters the Foron river course. As a result, the rail link runs into an open trench gallery composed of the Foron river alluvial deposits retaining a high and flowing groundwater table as is highlighted in Figure 1. The constructed gallery will result in a cut-off of the groundwater, which will have a significant impact of the safety of the structure if equilibrium of the groundwater is not restored.

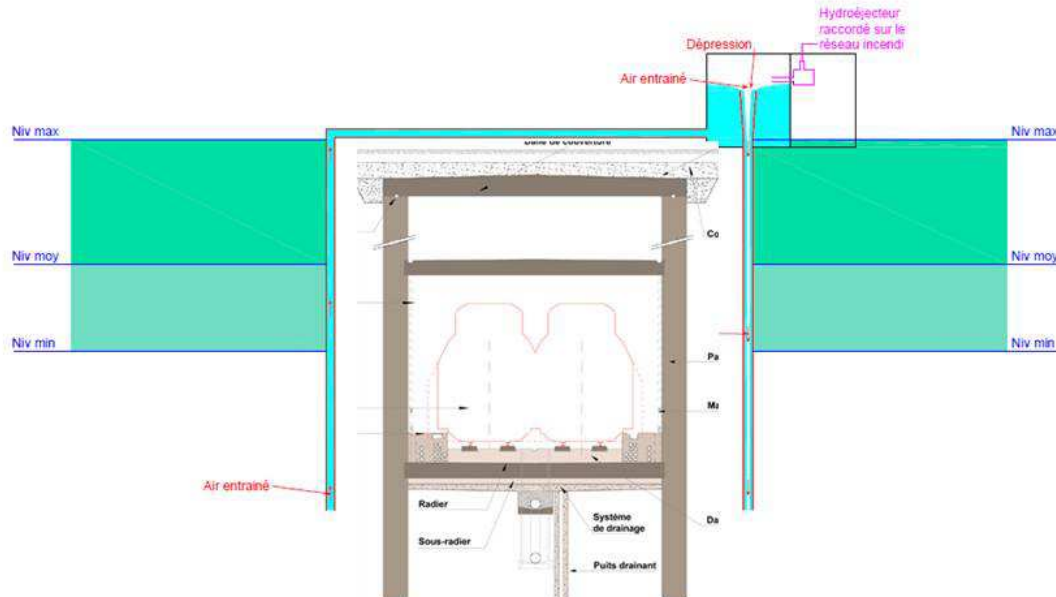


**Figure 1:** Cross section of the double track CEVA tunnel with the groundwater water transfer system connecting the two sides of the gallery.

In order to solve this issue and reequilibrate the groundwater levels on both sides of the tunnel, an innovative inverse self-priming system was proposed to convey the groundwater thus requiring no continuous pumping and energy requirements. The proposed inverse siphon uses a unique multiphase flow condition of both water and air permitted by a specialised vortex chamber installed in a variable pressure 'sealed box'. The purpose of the air-water flow conditions provided by the vortex is to render the system stall-free in the presence of air entrainment through faulty or damaged pipe work under future working conditions.

Owing to the novelty of such an approach to siphoning, as far as the authors are aware, there are no studies available conceiving a reliable design for the system, apart from some work on vortex chambers carried out by [1], [2], [3], [4] and [5] in the context of dropshafts for energy dissipation in sewers and hydropower plants. Furthermore, the previous studies were carried out for constant atmospheric pressure conditions, wherein the proposed vortex flow conditions within the sealed box are subject to variable negative pressure conditions. Therefore, a full-scale (1:1) physical model of the system was designed and constructed at the Laboratoire de Constructions Hydrauliques (LCH) of the EPFL, Switzerland. Simulations of such hydraulic structures at full-scale (or almost full-scale) prior to in-situ commissioning are regularly required to eliminate scale effects which would otherwise be present in a reduced scale model. Thus, by simulating an inverted siphon in a laboratory environment at full-scale, it was possible to undertake the following objectives as part of this study:

1. To characterize the initiation and stability conditions of the system.
2. To characterize the limiting operating conditions of the system in relation to the ground water table levels.
3. To determine the critical conditions of insufficient air entrainment by the downstream flow conditions.
4. To compare the performance data to existing hydraulic equations and draw conclusions on the effect of negative pressure on the flow system.

## 2. EXPERIMENTAL FACILITY

### 2.1 Physical model

The experimental facility reproduces the principal components of a self-primed siphon and the surrounding terrain. It is meant to transfer water above the CEVA tunnel in order to control the ground water table on both sides. Figure 2 shows a schematic representation of the main parts of the model. Different combinations of groundwater levels and discharges can be evaluated to quantify and assess the functioning of the siphon.

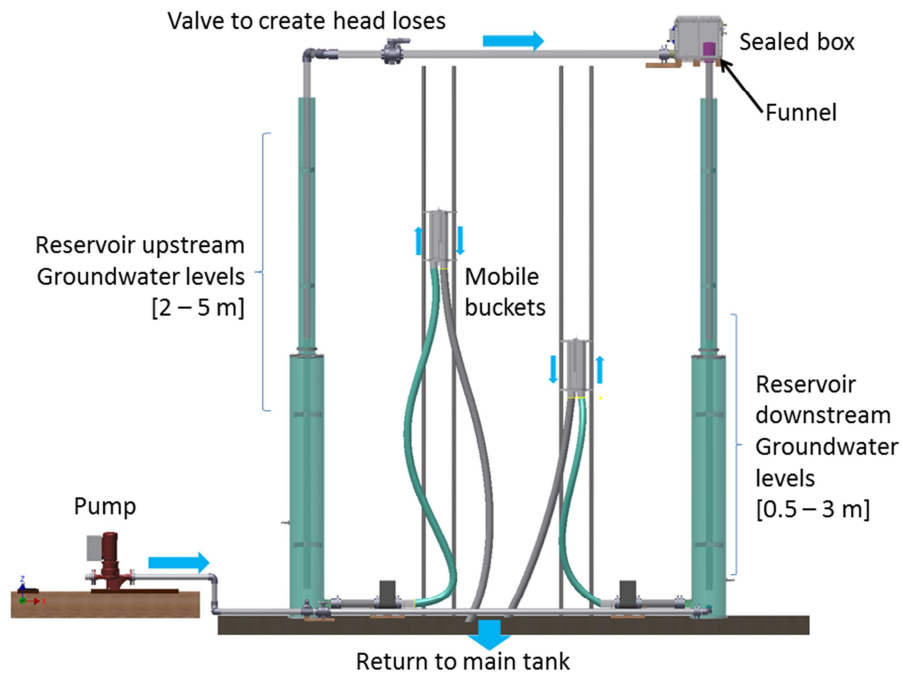


**Figure 2:** Schematic representation of the model built 1:1 scale of a self-primed siphon.

The study is carried out at 1:1 scale except for the horizontal conduit. The total height of the model is 6.40 m high and 5 m wide. The length of the horizontal pipe was reduced from 15 m in the prototype to 4.50 m in model. A spherical valve was used to simulate the range of head-losses expected in the full length pipe.

The upstream and downstream groundwater table levels are reproduced by large circular reservoirs supplied by a pump; levels are regulated by suspended movable buckets (overflow structures) which can be adjusted in height. The buckets were designed using a multiphase model in Flow3D for a maximum discharge of 9 l/s (Figure 3). The final design resulted in a cylinder of 0.21 m diameter and 0.50 m height. The pipe diameter for the inlet and outlet of the buckets was defined from the results of the numerical simulation. An internal wall made from PVC with a 0.20 m height is placed centrally in the bucket in order to separate the inlet and outlet. Internal tubes for air supply are included in the bucket system. The buckets are attached to a metallic cable and are movable by a motor (Figure 3). Each bucket can be moved individually and is handled with a manual control. A pump used to supply water to the system and the outlets of the buckets are connected to a main tank from the laboratory generating a closed circuit.

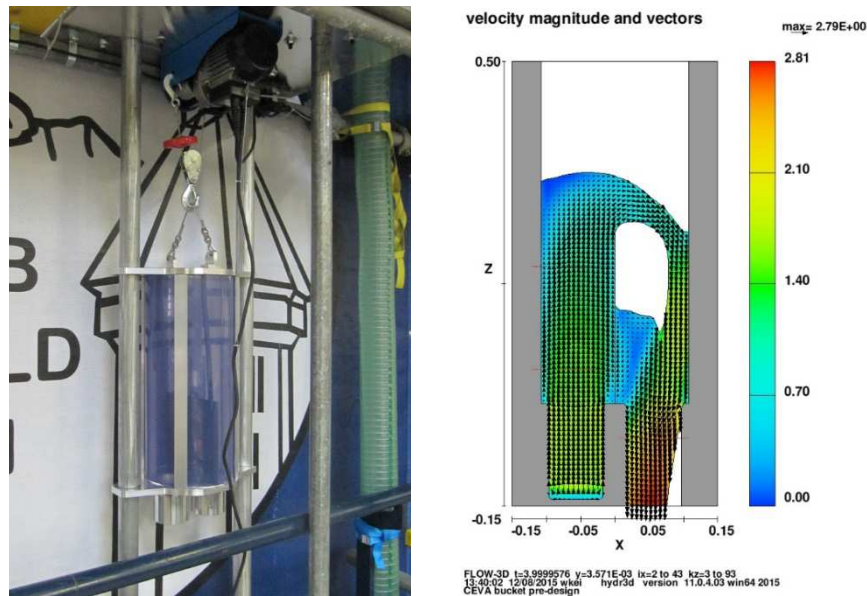


**Figure 3:** Image of the mobile bucket and the motor (left). Image of the numerical simulation done with Flow 3D (right).

From the main tank, water is pumped to both reservoirs (which simulate upstream and downstream water table levels) through a horizontal pipe with perforations to homogenise the incoming flow. Butterfly valves are installed upstream of the reservoirs to regulate discharge going to each reservoir wherein the reservoir depth is maintained by the buckets which effectively simulates the ground water level in real conditions. A 90 mm diameter vertical pipe is contained within the reservoir which serves the purpose of conveying water to the horizontal pipe section and subsequently to the main siphon components. A ‘sealed box’ comprises the main component of the siphon system which is located at the end of the horizontal section. The unique feature of the siphon is that it is a multiphase flow system; both air and water (free-surface flow) are permitted in the siphon without cessation of the siphon itself. This unique feature means that the siphon will not stall when air is permitted in the system (for example through inflow of additional air through faulty pipe connections or disturbed pipes in the future).

In order to provide a steady, multiphase flow of air and water simultaneously, use was made of the free-surface vortex where a concentrated region of vorticity results in a local depression of the free-surface, and under ideal conditions of circulation, air entrainment and flow of air through a full air core is maintained ([6]). In the sealed box, an off central vertical orifice connected to the downstream vertical pipe ensures that a steady rate of vorticity is generated in the box by asymmetry of the approach flow from the horizontal pipe (see [7] and [8]). This asymmetric hydraulic arrangement alone was not sufficient to provide enough circulation to maintain a stable vortex air core over the outlet and therefore an additional scroll type vortex chamber was added to ensure that vorticity is focused over the outlet. The scroll vortex chamber was designed according to the depth-discharge equations derived by [5] for subcritical approach flows. The scroll chamber walls had a logarithmic spiral geometry as outlined in Figure 6 wherein the geometry of the logarithmic walls were bounded by the size of the box. The sealed box has dimensions of 0.5 m long 0.5 m wide and 0.40 m high and manufactured from 6 Plexiglas plates joined by screws. The top plate can be removed for atmospheric pressure tests. It was designed to withstand a differential pressure of minus 10 m water column. In the left wall of the box, there are two air rotameters, a pressure sensor and the inlet connection from the horizontal pipe. In the right wall, there is a connection for a vacuum pump that is required to initiate the siphon. The funnel is connected to the downstream reservoir by a vertical pipe. For this model, two different sizes of funnels were constructed in the workshop of LCH. Both of them were cut out of a PVC block with the shape of a standard overflow spillway in order to improve the adherence of the jet. The design yielded vortex flows where the air core extended deep into the intake. The critical submergence (i.e. the height of vortex collapse) was observed for high discharges. The construction of the model in Plexiglas and transparent PVC permitted visualization during experiments.



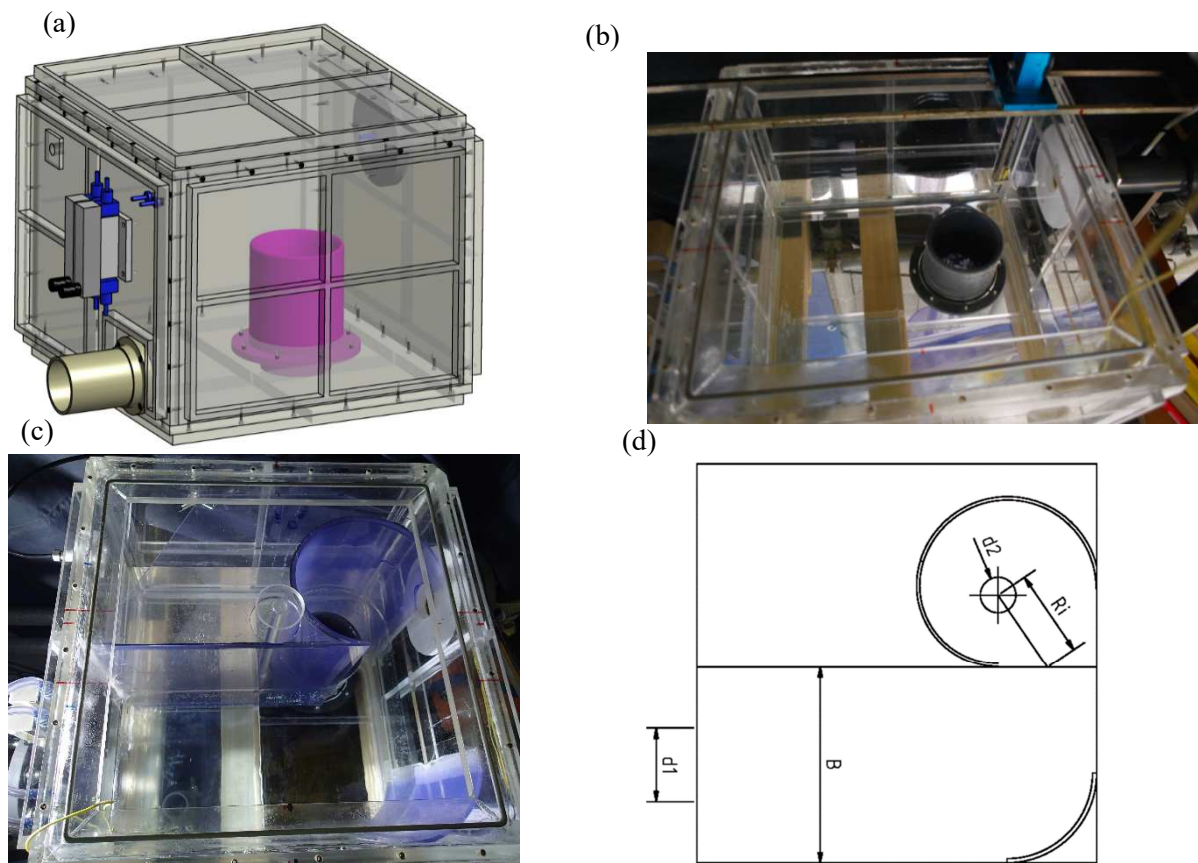


**Figure 4:** (a) 3D schematic drawing of the airtight box showing the position of the inlet and outlet funnel (b) image of the installed sealed box (c) adaptation with a scroll vortex chamber and (d) a line diagram outlining the main components of the logarithmic spiral geometry.

## 2.2 Hydraulic Similitude and Instrumentation

### 2.2.1 Hydraulic similitude

Due to the 1:1 scale, no scale effects are encountered. For this facility, it was necessary to retain 1:1 scale as the flow system depended of the effects of viscosity, surface tension and gravity simultaneously i.e. Froude similitude would not be applicable in the pressure conduit sections whereas Reynolds similitude would not be valid in the sealed box. Furthermore, variable air pressure in the sealed box added higher orders of complexity to the flow problem which rendered reduced scale modelling too risky.

### 2.2.2 Instrumentation

Two flowmeters are placed between the main reservoirs and the mobile buckets to regulate water discharge  $Q_W$ . Two air rotameters are connected to the airtight box to regulate and measure the required air flow  $Q_A$ . The position of all the instrumentation is shown in Figure 5.

The pressure inside the model is measured in various locations with vented gauge pressure transmitters. The main reservoirs have pressure sensors at 1.00 and 0.50 meters from the bottom (upstream and downstream respectively). By measuring the pressure inside the reservoirs, the water level inside the reservoir can be determined assuming a hydrostatic pressure distribution. In a lateral wall of the airtight box there is also a pressure sensor to measure the depression generated by the vacuum pump.

In order to know the  $Q - h$  relation for each funnel, various discharges were measured for atmospheric conditions. The water depth inside the box was measured with an electrical point gauge

allowing precise average water level measurement in a wavy environment. When the box is closed, there are graphical scales to read the water depth on the side walls. The measuring instruments are connected to a computer and through a LabVIEW acquisition program. With this configuration it is possible to record: discharge from both reservoirs, pressure inside both reservoirs and pressure inside the box and air flow at an acquisition frequency is 200 Hz.

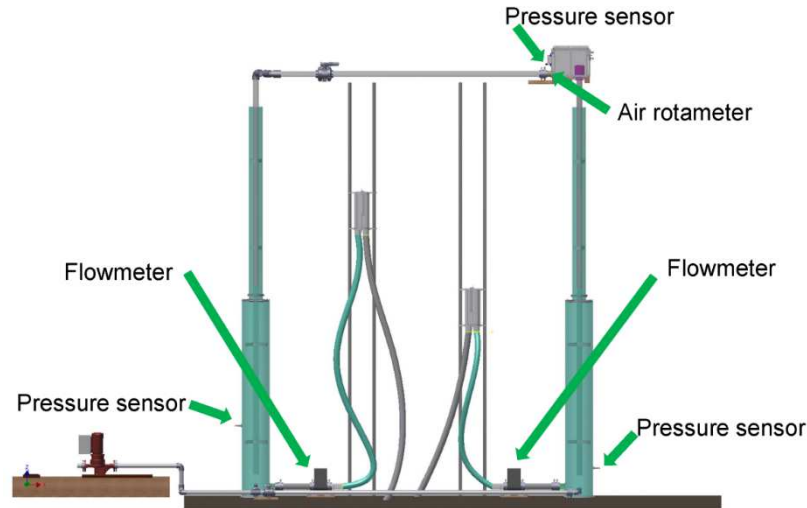


Figure 5: Schematic drawing with the instrumentation

### 3. PARAMETRIC STUDY

The main parameters under investigation are summarized in Table 1 with their respective range. Their position is visualized in Figure 6 and Figure 7. The physical model tests can be divided into three phases:

1. Tests with direct supply to the box under atmospheric pressure: this phase will allow characterizing the flow of the funnel (discharge, height of water). The box is connected directly to the fire network for water supply.
2. Tests with direct supply to the box with negative pressures: the box is closed in an airtight manner, making it possible to measure the flow of air carried by the flow with the aid of the rotameters.
3. Tests with priming of the siphon (by vacuum pump or venturi ejector functioning with the fire hose discharge): during this phase, the stability of the pre-primed siphon will be characterized as a function of the upstream / downstream levels as well as the height of water in the sealed box.

Symbol	Parameter	Instrument	Precision / error	Range	
				Min	Max
$H_1$	Upstream head	Vented Gauge Pressure Transmitter PR-25	max +/-0.5% full scale	0.05 bar	0.55 bar
$H_2$	Downstream head	Vented Gauge Pressure Transmitter PR-25	max +/-0.5% full scale	0.05 bar	0.55 bar
$Q_1$	Water discharge of tank upstream	Electromagnetic flow measuring system Proline Promag 50	<+/-0.5% above 10% of max discharge	0.7 l/s	10 l/s
$Q_2$	Water discharge of tank downstream	Electromagnetic flow measuring system Proline Promag 50	<+/-0.5% above 10% of max discharge	0 l/s	10 l/s
$Q_{fire}$	Water	Electromagnetic flow	<+/-0.5% above 10% of	average 1200 l/min	

	discharge of fire hose	measuring system Proline Promag 50	max discharge		
$P_{\text{fire}}$	Pressure fire hose	Gauge guard type Z700 PVC-U	Not mentioned		8-9 bar
$P_{\text{box}}$	Pressure inside box	Vented Gauge Pressure Transmitter PR-25	max +/-0.5% full scale	-0.6 bar	0
$Q_{\text{air}}$	Discharge of air into the box	Air rotameters x2	DK 800 2.5% to 50% of $Q_{\text{max}}$	20 l/h	3600 l/h
$h_{\text{box}}$	Water level inside box	Scale gauge (for the closed box)	$\approx 1 - 2$ mm, depending on the intensity of waves	0 m	0.40 m
$h_{\text{box}}$	Water level inside box	Electric resistance point gauge	Theoretical 0.1mm Practical +/-0.5mm, depending on the intensity of waves	0 m	0.40 m
$T_{\text{air}}$	Air temperature	Thermometer	-		
$T_{\text{w}}$	Water temperature	Thermometer	-		
t	Time	Chronometer	-		

**Table 1** List of parameters measured and instrumentation

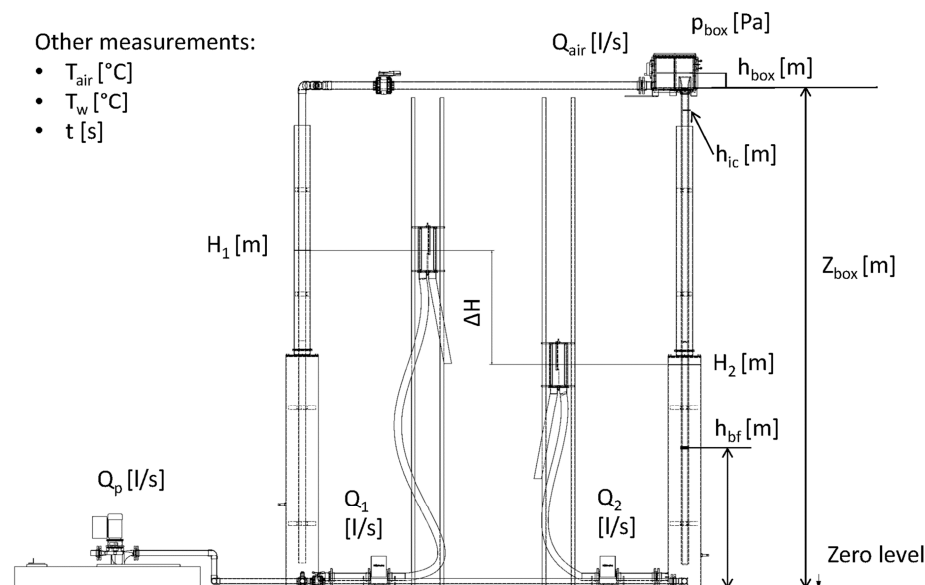


**Figure 6:** Schematic representation of parameters measured in the model

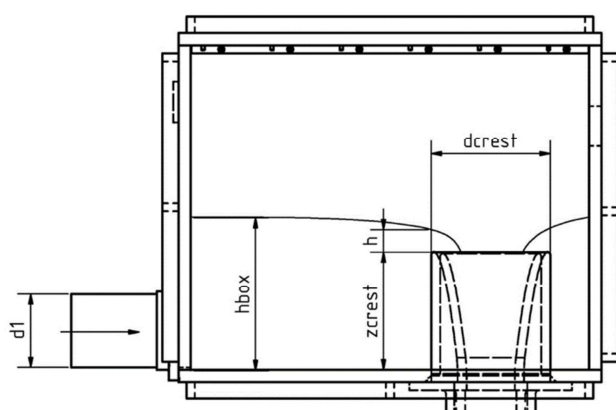


Figure 7: Schematic representation of parameters measured inside the airtight box – transversal view

## 4. RESULTS AND DISCUSSION

The main results can be introduced as follows:

- The depth-discharge relation for both funnels at free-surface under atmospheric pressure could be determined as a combination of free overfall structure and vortex induced flow similar to a morning glory spillway ([10]).
- The depth-discharge relationship for both funnels at negative pressure.
- Stability of free-surface vortex flow and performance limitations such as head differences and air supply.

### 4.1 Phase 1, depth-discharge at atmospheric pressure

The main objective of this phase was to characterize the flow conditions and the depth-discharge relation of the funnels. The firsts runs shows that the square initial design of the box induced a highly perturbed free surface, leading to downstream discharge instabilities and sometimes sudden closure (choking) of the impinging jet. The depth-discharge relation measured for the two sizes of funnels are shown in Figure 8. This figure also compares those measurements with the discharges computed with a classical weir equation (with a discharge coefficient of 0.44) and with the semi-empirical vortex equations as defined by [5] based on the approach flow geometry. As shown in Figure 8, there is a good agreement between the experimental and theoretical equations which are clearly divided by a transition point.

The transition point is characterised by two phases: (A) For low discharge, the weir approach is valid as the flow system is independent of the rotating flow conditions and (B) For higher discharges, the vortex approach fits well with the data, and the funnel is practically not perturbing the vortex flow.

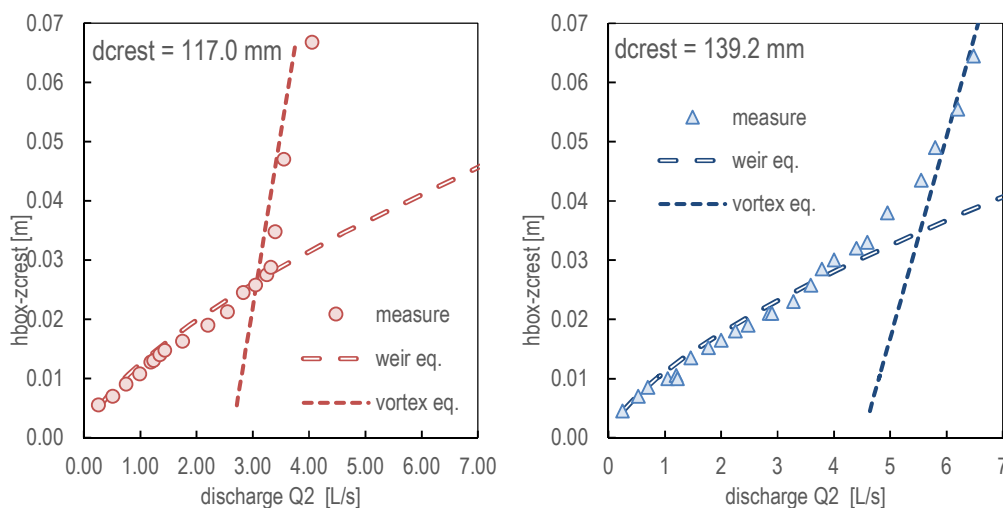


Figure 8: Depth-discharge relation for both funnels at free surface under atmospheric pressure, comparison with theoretical classical weir equation and with the vortex equation

### 4.1 Phase 2, depth-discharge at negative pressure

To determine the influence of the negative pressure inside the box, depth-discharge relations for both funnels at negative pressure were experimentally determined. The depth-discharge relationship was again measured for the small funnel with pressure inside the box varying from -0.018 bar to -0.157 bar as shown in Figure 9. As with the tests at atmospheric pressure, the experimental points agree well with the weir and vortex equations. No apparent influence of the negative pressure on the depth-discharge relation was observed for the range of negative pressure investigated. This finding was interesting as it states that (for the measured conditions) free-surface discharges in weirs and vortex



flows are independent of atmospheric pressures: thus the flows are only dependent on gravity and the approach flow conditions (see [5]) which can simplify the problem significantly in future analytical work.

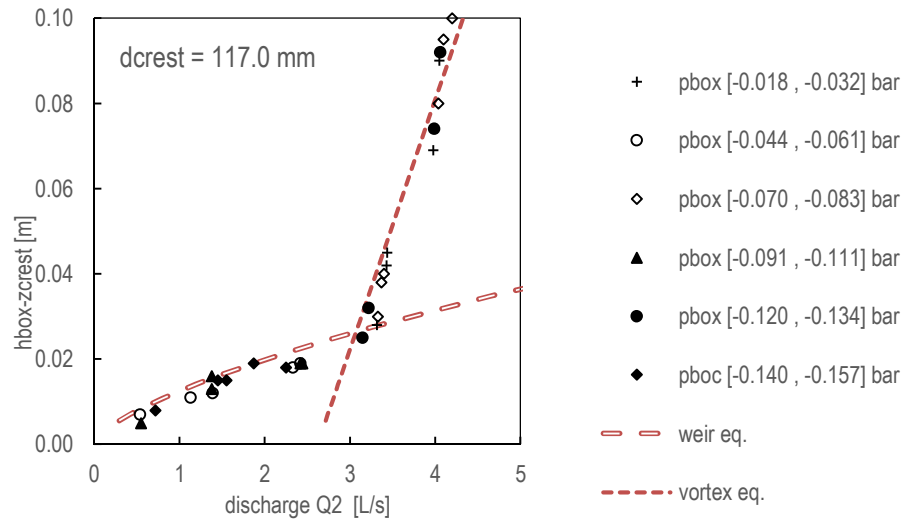


**Figure 9:** Depth-discharge relation for the small funnel at free surface under variable negative pressure inside the box, comparison with theoretical classical weir equation and with the vortex equation

#### 4.1 Phase 3, working limit for air entrainment

The main objective of this phase was to characterize the influence of air inflow on the discharge and ultimately the condition of siphon stall (cessation) or ‘loss of prime’. This part of the study was restricted to weir flow conditions.

An initial water discharge was set without air inflow ( $Q_{2i}$ ), the discharge  $Q_2$  was measured while the air inflow into the box ( $Q_{air}$ , measured at atmospheric pressure) was progressively increased. Figure 10 shows the discharge reduction of the system while air was allowed to enter into the siphon.

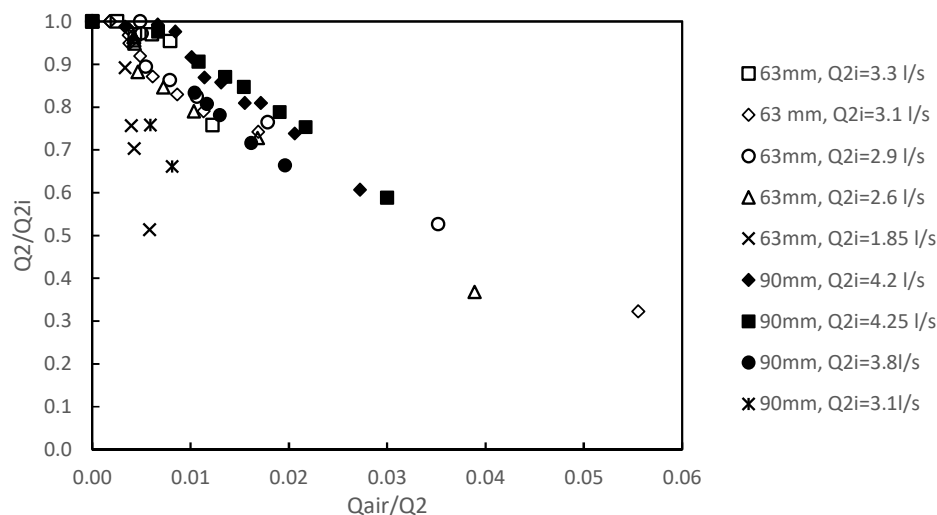


**Figure 10:** Relative air inflow and discharge reduction, for weir flow conditions and both funnels

Except for the lowest tested discharge per funnel, the discharge reductions follows a general trend which can be approximated by:

$$\frac{Q_2}{Q_{2i}} = \frac{1}{15} \frac{Q_{air}}{Q_2}$$

The loss of prime (or condition under which the siphon stalls) occurs when the water discharge is no longer of suitable magnitude to evacuate the air downstream. This occurs when the axial velocity in the downstream pipe is lower than approximately 0.4 m/s. This can be related to the buoyant velocity of air bubbles in water. According to [11], the raise velocity of an air bubble is approximately constant at 0.24 m/s for bubble diameters between 1.5 mm and 4.5 mm; and for a water pressure of less than 1 bar, the variation in bubble diameter is negligible. The main air evacuation parameter is air discharge. For the above mentioned tests with small discharge, the initial conditions were too close to this air evacuation limit, explaining the strong discharge reduction even with a very small air injection.

## 5. CONCLUSION

The study provided a full-scale simulation of a novel, multiphase self-priming siphon system which is to be installed on the CEVA project to maintain equilibrium of water tables. Full scale physical modelling was performed at LCH (EPFL) on the model with a 6.4 m × 5.0 m vertical foot-print. Full-scale simulation ensured that scale effects could be eliminated when transferring performance data to the in-situ system. The results showed that the depth-discharge relationship within the combined vortex chamber and funnel intake consisted of two relationships separated by a transition point. The two relationships agreed closely with available analytical models. The transition point occurred when rotational flow conditions dominated the weir flow under atmospheric conditions. For negative pressure conditions, the depth-discharge equations did not alter stating that free-surface weir and vortex flows are independent of pressure conditions and are only dependent on the approach flow geometry, at least for the range of negative pressures measured in this study. Finally, an empirical relationship for the air flow in the sealed box was defined. The results also suggest that the siphon will cease to operate (stall) when the water discharge is unable to evacuate air bubbles (i.e. maintain air flow) downstream of the intake.

## ACKNOWLEDGEMENTS

The presented study is financed by the Swiss Federal Railways as main stakeholder of the CEVA project.

## REFERENCES AND CITATIONS

- [1] Drioli, C. (1947). “Su un particolare tipo di imbocco per pozzi di scarico (scaricatore idraulico a vortice).” *L’Energia Elettrica*, 24(10), 447–452 (in Italian).
- [2] Ackers, P., and Crump, E. S. (1960). “The vortex drop.” *ICE Proc.*, 16(4), 433–442.
- [3] Jain, S.C. and Kennedy, J.F., 1983. Vortex-flow drop structures for the Milwaukee metropolitan sewerage district inline storage system (No. 264). Iowa Institute of Hydraulic Research, the University of Iowa.
- [4] Hager, W. H. (1985). “Head-discharge relation for vortex shaft.” *J. Hydraul. Eng.*, 10.1061/(ASCE)0733-9429(1985)111:6(1015), 1015–1020. Durgin, W.W. and Hecker, G.E., 1978, June. The modeling of vortices at intake structures. In *Proceedings of the ASCE/ASME/IAHR Joint Symposium on the Design and Operation of Fluid Machinery*, Fort Collins, Colo (pp. 12-14).
- [5] Mulligan, S., Casserly, J. and Sherlock, R., 2016. Effects of Geometry on Strong Free-Surface Vortices in Subcritical Approach Flows. *Journal of Hydraulic Engineering*, 142(11), p.04016051.
- [6] Knauss, J. E. (1987). *Swirling flow problems at intakes*, A. A. Balkema, Rotterdam, Netherlands.

- [7] Durgin, W.W. and Hecker, G.E., 1978, June. The modeling of vortices at intake structures. In Proceedings of the ASCE/ASME/IAHR Joint Symposium on the Design and Operation of Fluid Machinery, Fort Collins, Colo (pp. 12-14).
- [8] Mulligan, S., 2015. Experimental and numerical analysis of three-dimensional free-surface turbulent vortex flows with strong circulation. PhD Dissertation, IT Sligo.
- [9] Bradley, J.N., 1956. Morning-glory shaft spillways: a symposium: prototype behavior. Transactions of the American Society of Civil Engineers, 121(1), pp.312-333.
- [10] Leifer I., Patro R. K., and Bowyer P. (2000). A study on the temperature variation of rise velocity for large clean bubbles, Journal of Atmospheric and Oceanic Technology, 17(10), 1392-1402.